Chin. J. Astron. Astrophys. Vol. 1, No. 2, (2001) 161–175
(http://www.chjaa.org or http://chjaa.bao.ac.cn)

Chinese Journal of
Astronomy and
Astrophysics

On the Line Formation in Stellar Magnetized Atmospheres

Zhong-Quan Qu[1,2⋆], Xiao-Yu Zhang[1] and Zhi Xu[1]

[1]Yunnan Observatory, Chinese Academy of Sciences, Kunming 650011
[2] National Astronomical Observatories, Chinese Academy of Sciences, Beijing 100012

Received 2000 December 14; accepted 2001 January 4

Abstract The line formation process in stellar magnetized atmospheres is studied by observing the wavelength-dependence of Stokes contribution functions. The influence of magnetic field on the escape line photon distribution and line absorption is obtained by comparing with the null magnetic field case. Two models are adopted. One assumes limited distributions of both the line absorption and magnetic field where a hypothetical magneto-sensitive line is formed. The other is a model atmosphere of sunspot umbra in which Mg I 5172.7 forms. It is found that the magnetic field influences the formation region of Stokes I at wavelengths sufficient close to the Zeeman splitting points $\pm\Delta\lambda_H$. The formation regions at wavelengths far away from the Zeeman splitting points generally show a non-magnetic behaviour. Further, if the line core is split by the Zeeman effect, the line formation core introduced in the previous paper disappears. On the other hand, Stokes Q, U, V at each wavelength within the line form in the same layers where both the line absorption and magnetic field are present in the models accepted for the lines used. When the line absorption and magnetic field ubiquitously exist, the formation regions of the π peaks or valleys of Stokes Q, U and those of σ of Stokes V generally cover the widest depth range. It is pointed out that such a study is instructive in the explanation of solar polarized filtergrams. It can tell us at each observation point where the received line photons of wavelengths within the bandpass come from and where their polarization states are formed or give us the distributions of these photons as well as their polarization intensities. Thus a three-dimensional image can be constructed for a morphologic study of the observed area from serial filtergrams.

Key words: line: formation – radiative transfer – Sun: atmosphere – sunspots – Sun: magnetic fields

⋆ E-mail: ssg@public.km.yn.cn

1 INTRODUCTION

In the previous paper (Qu et al. 1999, hereafter Paper I), we investigated the wavelength-dependence of four contribution functions (CFs) derived from different formal solutions and referring to different emergent quantities in the unpolarized case. Because one cannot generally assign a single formation region to the whole line band in a real stellar atmosphere, e.g., the solar atmosphere, instead, the line formation region can be defined as the layers deviating farthest from the stellar atmospheric layers where thermalization prevails. These are the layers where the line core with depth-averaged Doppler width forms. Thus the concept of line formation core was introduced to represent one important aspect of line formation property. However, it should be noted that the line formation core is not equivalent to the simple line core. As will be seen, if the line splitting induced by the Zeeman effect occurs in the line core, the line formation core will disappear while the line core always exists as a concept only related to the wavelength interval division of a spectral line.

In this paper, we extend the investigation to the Stokes spectra (the wavelength distribution of specific and polarization intensities) formation issue both in partially and ubiquitously magnetized atmospheres. To conveniently evaluate the role of magnetic field in the line formation process, we directly add the field stratification into the model atmospheres used in Paper I. As is well known, the introduction of magnetic fields into the atmosphere can change its physical state, e.g., the level populations of the relevant atoms or ions and the pressure equilibrium. But this effect does not generally alter the state so much that the atmospheric parameters are critically changed, if the field strength is not as strong in stellar atmospheres as in the solar chromosphere and photosphere. On the other hand, one may think from another point of view that the introduction of magnetic field changes some original physical state to the current one described by the accepted model atmosphere.

In the following discussion, we stress the following questions and try to give some suitable answers.

(1) Does the formation region of the line core still keep its properties that can be used to define the line formation region in the presence of magnetic field?

(2) Are the formation regions of Stokes I of all the wavelengths, or only some of them, affected?

(3) What is the meaning of the formation regions of Stokes Q, U and V? Can the formation regions of their peaks or valleys in the line wings (signifying π- or σ-components respectively) represent the Stokes profile formation regions?

(4) Do all the Stokes polarization components of the same wavelength form in the same region?

Many researchers have speculated the influence of magnetic field on the line formation height (refer to Qu (1997) for a detailed review). For example, Larsson, Solanki and Grossmann-Doerth (1990) emphasized the influence of different flux tube parameters on the height of formation in order to ensure a better understanding of the diagnostics on temperature and magnetic field. About the role of magnetic field, they concluded that an increase in the longitudinal field strength makes the line center form deeper while the formation heights of line flanks increase until the line is completely split. Generally, when the Zeeman splitting becomes larger than the line width, the formation heights are strongly affected by the field strengths.

Nevertheless, the effort to apply the formation height in the physical quantity diagnostics

is demonstrated to be somewhat misleading, as Sánchez Almeida (1996) pointed out, the line formation height derived from the CFs cannot be assigned to a "formation height of a measurement" for such physical quantities as vector magnetic field by analyzing the measured Stokes profiles. But this assignment can be done by the Response Function (RF) (also refer to Ruiz Cobo & del Toro Iniesta 1994). We (Qu & Gu 1999) have given an equation to show that one cannot equate a "line formation height" to a "height of a measurement". But all these do not mean that a line formation theory depending on the CFs is of no use. The theory can at least help us to better understand the line formation process in stellar atmosphere and gives a great help to understand the solar filtergrams, as briefly discussed in the paper.

2 STOKES CONTRIBUTION FUNCTIONS

In Paper I, we selected four CFs to two emergent quantities, namely, specific intensity and relative line depression. They were derived from differential and integral formal solutions to radiative transfer equation, respectively. What we concluded in the paper is that if one distinguishes between the meanings of the CFs to the intensity and relative line depression, the information on the line formation region can be supplied by any reasonable CF in the sense that its depth integral should be proportional to the corresponding emergent quantity. Many CFs in the polarized case are proposed in the literature. For consistency with Paper I, we adopt the more easily calculable ones generalized from those in the unpolarized case.

The polarized radiative or Stokes transfer equations can be written as (see Landi Degl' Innocenti 1976, but with some symbols changed)

$$\begin{aligned}
\mathrm{d}I/\mathrm{d}z = \; & -\kappa_c(I-S_c)-\kappa_l\phi_I(I-S_l) \\
& -\kappa_l\phi_Q Q-\kappa_l\phi_U U-\kappa_l\phi_V V; \\
\mathrm{d}Q/\mathrm{d}z = \; & -\kappa_l\phi_Q(I-S_l)-\kappa_l\phi_I Q-\kappa_l\phi_V^{'}U+\kappa_l\phi_U^{'}V; \\
\mathrm{d}U/\mathrm{d}z = \; & -\kappa_l\phi_U(I-S_l)-\kappa_l\phi_I U-\kappa_l\phi_Q^{'}V+\kappa_l\phi_V^{'}Q; \\
\mathrm{d}V/\mathrm{d}z = \; & -\kappa_l\phi_V(I-S_l)-\kappa_l\phi_I V-\kappa_l\phi_U^{'}Q+\kappa_l\phi_Q^{'}U.
\end{aligned} \tag{1}$$

Where the geometric height z is measured along the line of sight; I, Q, U, V are the Stokes parameters; κ_l and κ_c indicate the line-center and continuum absorption coefficients; S_l and S_c stand for the line and continuum source functions. $\phi_{I,Q,U,V}$ are the absorption profiles for the indicated Stokes parameters while $\phi^{'}_{Q,U,V}$ are the profiles that evaluate the magneto-optical effect. Their expressions can be found in Landi Degl'Innocenti (1976).

From the above equations, one can easily find that if there is no line absorption ($\kappa_l = 0$) or if magnetic field is absent (leading to $\phi_{Q,U,V}, \phi^{'}_{Q,U,V} = 0$) in the atmospheric layers, the Stokes polarization components Q, U, V will either be zero, or stay constant if they are produced below the considered layers. This reveals the necessary condition for confining the formation regions of these parameters.

Our formal solution procedure (see Paper I) can also be generalized to obtain the solutions to equation set (1). Like Rees et al. (1989, hereafter RMD), rewriting Eq.(1) in vector form,

$$\frac{\mathrm{d}\boldsymbol{I}}{\mathrm{d}z} = -\boldsymbol{K}\boldsymbol{I} + \boldsymbol{j} \tag{2}$$

and again in an even more compact form,

$$\frac{\mathrm{d}\boldsymbol{I}}{\mathrm{d}\tau} = \boldsymbol{I} - \boldsymbol{S}, \tag{3}$$

one can apply the procedure described in Paper I to get the formal solution

$$\boldsymbol{I}(\tau_k) = O_{0,k}\boldsymbol{I}(\tau_{k+1}) + O_k\boldsymbol{S}(\tau_{k+1}). \tag{4}$$

Where $O_{0,k}$ and O_k are the same operators expressed in equation (15) of Paper I. In Eqs. (2)–(3), $\boldsymbol{I} = (I, Q, U, V)^\dagger$ is Stokes formal vector († means transpose), $\boldsymbol{K}$ the 4×4 total absorption matrix

$$\begin{aligned} \boldsymbol{K} &= \kappa_c\mathbf{1} + \kappa_l \begin{pmatrix} \phi_I & \phi_Q & \phi_U & \phi_V \\ \phi_Q & \phi_I & \phi_V^{'} & -\phi_U^{'} \\ \phi_U & -\phi_V^{'} & \phi_I & \phi_Q^{'} \\ \phi_V & \phi_U^{'} & -\phi_Q^{'} & \phi_I \end{pmatrix} \\ &\equiv \kappa_c\mathbf{1} + \kappa_l\boldsymbol{\Phi}, \end{aligned} \tag{5}$$

$\mathbf{1}$ stands for the unit matrix of 4×4 , and $\boldsymbol{j}$ the 4×1 total emission vector

$$\boldsymbol{j} = (\kappa_c S_c\mathbf{1} + \kappa_l S_l\boldsymbol{\Phi})\boldsymbol{e}_0, \;\; \boldsymbol{e}_0 = (1, 0, 0, 0)^\dagger, \tag{6}$$

and $\boldsymbol{S}$ denotes the modified source function vector,

$$\boldsymbol{S} = \boldsymbol{j}/\kappa_I - (\boldsymbol{K}/\kappa_I - \mathbf{1})\boldsymbol{I}, \tag{7}$$

whereas $\kappa_I (= \kappa_c + \kappa_l\phi_I)$ is one of the equal diagonal elements of the total absorption matrix $\boldsymbol{K}$. It also defines the optical depth τ appearing in Eq.(3) as

$$\mathrm{d}\tau = -\kappa_I \mathrm{d}z. \tag{8}$$

Now, if one adopts the approximation

$$\frac{\mathrm{d}\boldsymbol{I}}{\mathrm{d}\tau}(\tau_k) = \frac{\boldsymbol{I}(\tau_{k+1}) - \boldsymbol{I}(\tau_k)}{\tau_{k+1} - \tau_k}, \tag{9}$$

and omits the higher-order derivative terms in Eq.(4), one obtains the famous DELO (Diagnal Element Lambda Operator) solution after several algebraic steps:

$$\boldsymbol{I}(\tau_k) = \boldsymbol{P}_k + \boldsymbol{Q}_k\boldsymbol{I}(\tau_{k+1}), \tag{10}$$

which was first given by RMD who used the integral formal solution to Eq.(3). It should be noted that RMD made the essentially same assumption as Eq.(9), for if we take the derivative with respect to τ of their assumption (64) about the depth variation of the total source function vector $\boldsymbol{S}$ we get Eq.(9). Adopting the same method, the solution to the transfer equation for the Stokes depression vector $\boldsymbol{R} = (1 - I/I_c, -Q/I_c, -U/I_c, -V/I_c)^\dagger$ can be derived. The corresponding opacity τ_R, source function vector $\boldsymbol{S}_R$ were also expressed in RMD. Note that solution (10) is also utilized to produce the Stokes profiles in the next section.

Though we adopt the DELO solution, the contribution functions to the emergent Stokes parameters or $\boldsymbol{R}$ defined by RMD is not so reasonable. Because, by numerical test, their depth integral of Stokes I at far line wings is much less than at other wavelengths within the line band, e.g., the line core, in the case of absorption line which we consider throughout this paper. To obtain proper CFs, we first derive the surface solution by iteration of Eq.(10) (the atmosphere is stratified by n grid points from the surface $n = 1$ to the bottom of the photosphere)

$$\begin{aligned} \boldsymbol{I}(\tau_1) = \; & \boldsymbol{P}_{1,1}^{'}\boldsymbol{S}_1 + (\boldsymbol{P}_{2,1}^{'} + \boldsymbol{Q}_1\boldsymbol{P}_{1,2}^{'})\boldsymbol{S}_2 \\ & + \boldsymbol{Q}_1(\boldsymbol{P}_{2,2}^{'} + \boldsymbol{Q}_2\boldsymbol{P}_{1,3}^{'})\boldsymbol{S}_3 + \cdots \\ & + \boldsymbol{Q}_1\boldsymbol{Q}_2\cdots\boldsymbol{Q}_{k-2}(\boldsymbol{P}_{2,k-1}^{'} + \boldsymbol{Q}_{k-1}\boldsymbol{P}_{1,k}^{'})\boldsymbol{S}_k + \cdots \\ & + \boldsymbol{Q}_1\boldsymbol{Q}_2\cdots\boldsymbol{Q}_{n-2}(\boldsymbol{P}_{2,n-1}^{'} + \boldsymbol{Q}_{n-1}\boldsymbol{P}_{1,n}^{'})\boldsymbol{S}_n, \end{aligned} \tag{11}$$

here

$$\begin{aligned} \boldsymbol{P}^{'}_{1,k} &= [\mathbf{1} + (F_k - G_k)\boldsymbol{K}^{'}_k]^{-1}(F_k - G_k); \\ \boldsymbol{P}^{'}_{2,k} &= [\mathbf{1} + (F_k - G_k)\boldsymbol{K}^{'}_k]^{-1}G_k \end{aligned} \tag{12}$$

and F_k, G_k are functions of the opacity τ expressed by equation (67) of RMD. The CFs to the emergent Stokes vector from the layer (τ_{k-1}, τ_k) is written as

$$\mathrm{CF}_{\boldsymbol{I}}(\tau_k) = \boldsymbol{Q}_1\boldsymbol{Q}_2\cdots\boldsymbol{Q}_{k-2}(\boldsymbol{P}^{'}_{2,k-1} + \boldsymbol{Q}_{k-1}\boldsymbol{P}^{'}_{1,k})\boldsymbol{S}_k. \tag{13}$$

Similarly, for the CFs to the emergent Stokes depression vector,

$$\mathrm{CF}_{R;\boldsymbol{I}}(\tau_k) = \boldsymbol{Q}_{R;1}\boldsymbol{Q}_{R;2}\cdots\boldsymbol{Q}_{R;k-2} \times (\boldsymbol{P}^{'}_{R;2,k-1} + \boldsymbol{Q}_{R;k-1}\boldsymbol{P}^{'}_{R;1,k})\boldsymbol{S}_{R;k}. \tag{14}$$

The above quantities with subscript R represent the counterparts of those quantities without the subscript appearing in the Stokes transfer equations and their solution (RMD), for there is one to one correspondence between the solutions of $\boldsymbol{I}$ and $\boldsymbol{R}$.

Physically, the magnetic field influences the specific intensity emerging from the atmosphere by changing the line absorption profile (γ denotes the field inclination angle, and here only the Zeeman triplet is considered) to

$$\phi_I = \frac{1}{2}H(v,a)\sin^2\gamma + \frac{1}{4}[H(v+v_H,a) + H(v-v_H),a](1+\cos^2\gamma)\,. \tag{15}$$

Similarly, the effect on Q, U, V is the appearance of their non-zero absorption profiles ϕ_Q, ϕ_U and ϕ_V. In the above equation, $H(v,a)$ is the Voigt function

$$H(v,a) = \frac{a}{\pi}\int\limits_{-\infty}^{\infty}\frac{e^{-t^2}}{(v-t)^2+a^2}dt \tag{16}$$

and

$$a = \Gamma/\Delta\lambda_D,\ \ v = \Delta\lambda/\Delta\lambda_D,\ \ v_H = \Delta\lambda_H/\Delta\lambda_D. \tag{17}$$

Γ is the damping constant, $\Delta\lambda$ stands for the wavelength displacement from the line center, $\Delta\lambda_H$, the Zeeman splitting and $\Delta\lambda_D$, the Doppler width. It is worth noting that the absorption profile variation by magnetic field at atmospheric layers leads directly to the variation of the opacity, and hence results in a depth migration of escape line photons. Thus, a change of line formation region occurs.

3 WAVELENGTH-DEPENDENCE OF STOKES CONTRIBUTION FUNCTIONS

The contribution function is created to describe the contribution of given stellar atmospheric layers to a surface quantity and, as pointed out in Paper I, the Stokes I formation region should be assigned to those levels from which the amount of escape line photons is dominant when the line absorption is ubiquitous according to CF_I, or those layers where the line absorption dominates according to CF_R. By generalizing this concept to the polarized case where the continuum is assumed to be unpolarized, the Stokes Q, U and V describe the polarization intensity carried by the escape line photons, the formation regions of Stokes Q, U and V should be those places where the escape line photons gain their dominant contribution of the corresponding polarization intensity due to the presence of magnetic field and line absorption according to $\mathrm{CF}_{\boldsymbol{I}}$, or where the Zeeman effect as well as the magneto-optical effect makes a dominant contribution to the corresponding polarization states according to $\mathrm{CF}_{R,\boldsymbol{I}}$.

3.1 Artificial Model Atmosphere

In order to find suitable answers to the questions listed in the first section, some simple model atmosphere is designed in the polarized case (also done by Larsson et al. 1990). Here we adopt an artificial non-LTE model atmosphere in which the atmosphere is stratified into only 11 layers (hereafter the "11-layer model ") from $z = 0$ (bottom) to 300 (surface) in step of 30 in unit of arbitrary length, and the line absorption is distributed from $z = 150(n = 6)$ to the surface $z = 300(n = 1)$. Fig. 1 plots the stratification of the logarithms of the damping constant a, Doppler width $\Delta\lambda_D$, line center absorption κ_l, continuum absorption κ_c, line source function S_l and continuum source function S_c, normalized respectively by their maximum values along the depth. The null magnetic field CF_I and $\mathrm{CF}_{R;I}$ curves of sample wavelengths are drawn in Fig. 2, to be compared with those when the magnetic field is inserted. Though the $\mathrm{CF}_{R;I}$ shows directly where the line absorption takes place, one may notice the similarity of those curves of both CFs at each of the sample wavelengths above the level $z = 180$ (the amplitude of $\mathrm{CF}_{R;I}$ curve of 180 mÅ is too small to be seen). It manifests that when the line absorption is present, the main factor in the determination of the CFs is the attenuation factor $e^{-\tau}$, which reflects the total absorption from the layer considered to the surface. In fact, the CF_I tells us the amount of the escape line photons from the layer while the $\mathrm{CF}_{R;I}$ informs us the magnitude of the line

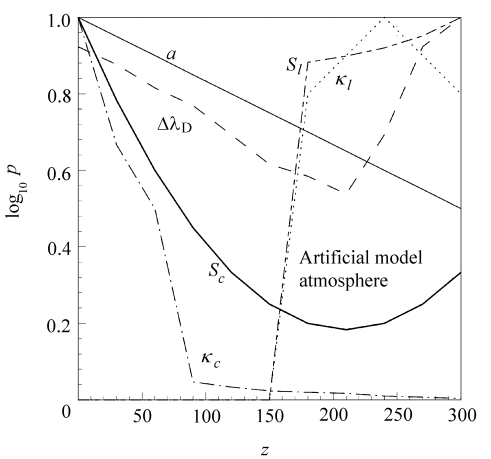

Fig. 1 The artificial model atmosphere. The curves represent distribution of logarithms of $p = a/a_{\max}$ (solid line), $\Delta\lambda_D/\Delta\lambda_{D,\max}$ (dashed line), $\kappa_l/\kappa_{l,\max}$ (dotted line), $\kappa_c/\kappa_{c,\max}$ (dash-dotted line), $S_l/S_{l,\max}$ (long-short line), and $S_c/S_{c,\max}$ (thick solid line), respectively.

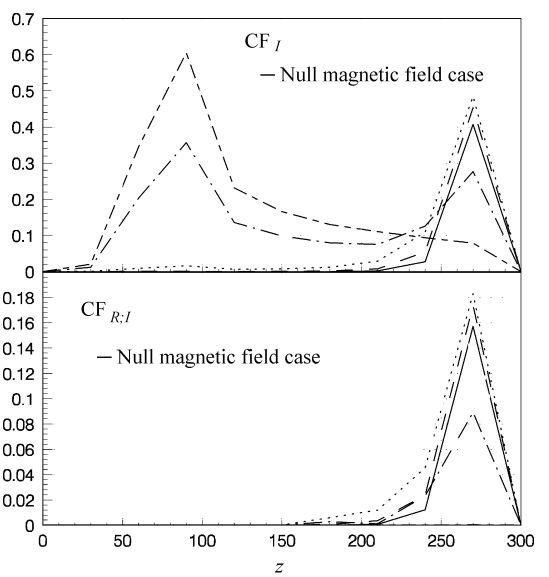

Fig. 2 The CF_I and $\mathrm{CF}_{R;I}$ curves at sample wavelengths. The types of curves correspond to CF curves at wavelength displacements from line center respectively: 0 mÅ (thin solid line); 30 mÅ (dashed line); 50 mÅ (dotted line); 90 mÅ (dash-dotted line); and 180 mÅ (long-short line). Note that the amplitude of $\mathrm{CF}_{R;I}$ at 180 mÅ is so small that the curve can hardly be seen.

absorption from the layer to the surface, multiplied by the absorption at the layer. In other word, the CF curves describe the depth distribution of the escape line photons while the $\mathrm{CF}_{R;I}$ curves give the depth distribution of the line absorption. Under the condition of complete frequency redistribution, they behave similarly if line absorption exists.

Now a constant magnetic field (1500 G, 60°, 30°) is inserted at grid points $z = 180$, 150, 120, 90, covering parts of layers both with and without line absorption. A magneto-sensitive line with Landé factor $g_{\mathrm{eff}} = 3.0$ is assumed to form in this tenuous atmosphere. Note that the layout of the magnetic stratification means that magnetic field is also present in two depth intervals from $z = 60(n = 9)$ to $z = 90(n = 8)$ and from $z = 180(n = 5)$ to $z = 210(n = 4)$. It is worth noting that studying the line formation in this model atmosphere and magnetic stratification supplies some clues on line formation process in a canopy-like magnetic field, which is frequently met in stellar penumbrae and solar small-scale magnetic features.

In Fig. 3, we plot the two kinds of CF curves. Comparing CF_I and $\mathrm{CF}_{R;I}$ to the null magnetic case, it is easily found that within $|\Delta\lambda| = 50\,\mathrm{m\AA}$ (dotted lines), the distribution of the escape line photons and the line absorption are not altered, or the line absorption is not changed. This also means that the width of the line formation core is not altered. The most significant effect of the magnetic field lies at the wavelengths ranging from $|\Delta\lambda| = 60\,\mathrm{m\AA}$ to 160 mÅ. For example, at 90 mÅ, some amount of escape line photons shift from deeper to shallower layers up to $z = 240$ (from CF_I). This reflects the line absorption variation in the layers (150, 210) where both the magnetic field and line absorption are present (from $\mathrm{CF}_{R;I}$). Beyond 160 mÅ (say 180 mÅ, long-short line), the curves also show the null magnetic field behaviour. From this fact, one can infer that the magnetic field cannot influence the formation regions of those wavelengths that are far away from the Zeeman splitting points ($|\Delta\lambda_H| = 119.1\,\mathrm{m\AA}$ in this case), or, in other words, line absorption variation due to magnetic field occurs only within a limited wavelength interval. This can be understood from the properties of the Voigt and Faraday functions.

From the sample curves of the two kinds of CF plotted in the other panels of Fig. 3, it is outstanding that the Stokes Q, U, V formation regions depend on both the magnetic field and line absorption. However, the role of the magnetic field looks like the line absorption in the unpolarized case. For example, above $z = 210$ where there is no magnetic field, there is no contribution. On the other hand, one may notice from $\mathrm{CF}_{Q,U,V}$ that the levels below depth $z = 60$, where the magnetic field is also assumed to be null, also contribute significantly to the surface Stokes Q, U, V. At first glance, it seems to indicate that the formation regions of emergent Stokes Q, U, V should contain this region; but it actually tells us that the escape photons emitted from those layers do go through the levels where magnetic field is present, and in this way the photons gain their polarization states. Therefore we should distinguish the place where the escape line photons are polarized from the place where they are produced. A similar situation was met by Larsson et al.(1990), but they only gave a mathematical explanation in terms of the density matrix. Hence the $\mathrm{CF}_{Q,U,V}$ cannot tell directly where magnetic field gives rise to the polarization states of the escape photons, i.e., the Stokes Q, U, V formation regions. However, there are some clues. There is a depth turning point $z = 150$, above which the polarization states begin to switch over to the opposite states in all three Stokes polarization CFs. This depth is just the point below which there is no line absorption and above which there is. It seems that those photons come from below the depth point experience the direct Zeeman effect. This may give an answer to the question, how to determine the lower boundary of the formation regions of the Stokes polarization parameters according to $\mathrm{CF}_{Q,U,V}$. Another

feature can be easily found that all the wavelengths of the Stokes Q, U, V form in the same region from $z = 150$ to 210, according to the above analysis. It can be seen from the $\mathrm{CF}_{Q,U,V}$ plots that the polarized escape line photons come mostly from below the layers where there is no line absorption. This clue cannot be found from the curves of $\mathrm{CF}_{R;Q,U}$. Evidently, all the polarized escape photons form in the same region regardless of their wavelengths or polarization states (linear or circular polarization state).

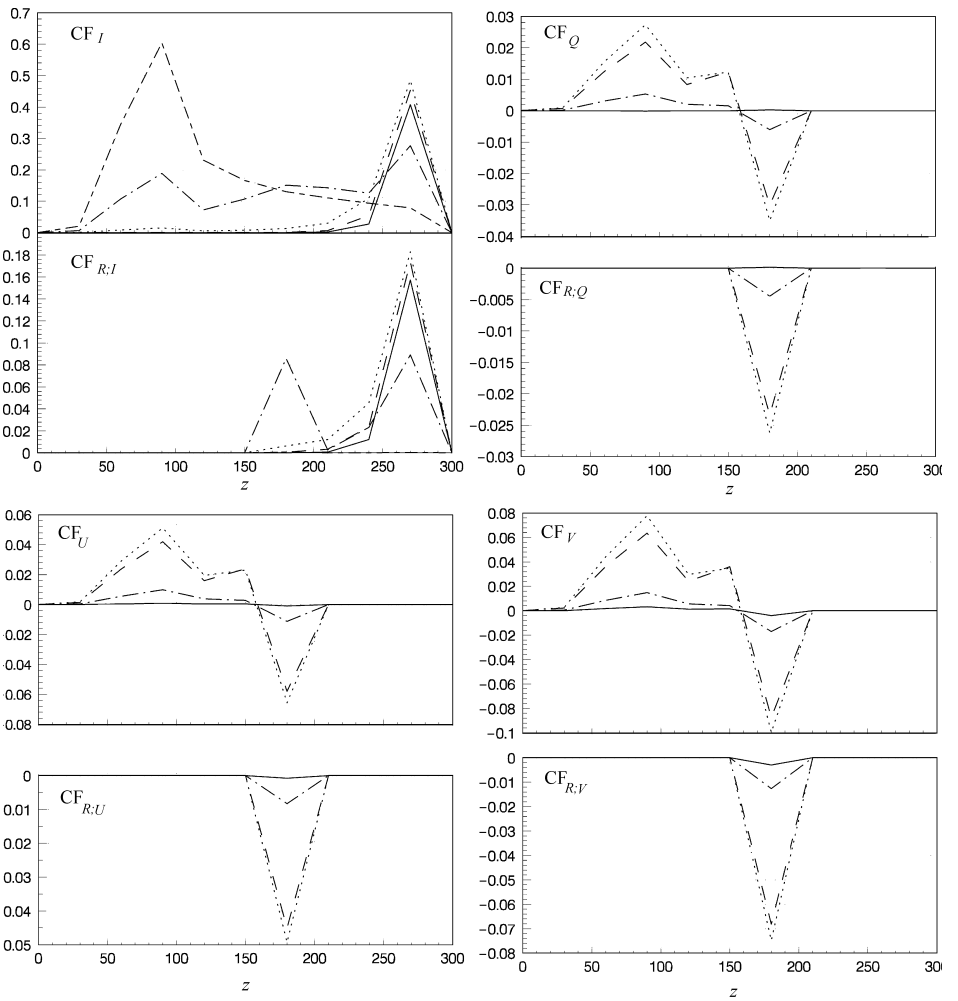

Fig. 3 The wavelength-dependence of sample Stokes CF and $\mathrm{CF}_{R;I}$ curves produced in an artificial teneous atmosphere with a weak field ($\boldsymbol{H} = (1500\,\mathrm{G}, 60°, 30°)$). The unit of $\mathrm{CF}_{I,Q,U,V}$ is the same as that of intensity and the $\mathrm{CF}_{R;I,Q,U,V}$ is dimensionless. Height is in arbitrary unit. The types of curves corresponding to CF_I and $\mathrm{CF}_{R;I}$ at wavelength displacements from line center respectively are the same as in Fig. 2. Those to $\mathrm{CF}_{Q,U,V}$ and $\mathrm{CF}_{R;Q,U,V}$ are: 50 mÅ (thin solid line); 90 mÅ (dashed line); 110 mÅ (dotted line); 150 mÅ (dash-dotted line). Note that Stokes Q, U and V form in the same region while Stokes I does not own this property in both CF and CF_R curves.

3.2 Mg I 5172.7 Solar Umbra Model Atmosphere

In the above model, we assume a restricted level distribution of both the line absorption and magnetic field. It is shown that the formation regions of Stokes Q, U and V are the same for all the wavelengths within the line band, and agree completely with the domain where both line absorption and magnetic field are present, while the formation regions of Stokes I are different and are wavelength dependent. But how about the situation where both factors are ubiquitous and the atmosphere is opaque, as in sunspot umbra? In such a case, one cannot simply assign the formation regions of Stokes polarization components to the regions defined above. The only way to get the information is to evaluate the relative contributions from the different layers. For this more detailed exploration, the Mg I 5172.7 ($g_{\rm eff} = 1.75$) model atmosphere of sunspot umbra (used originally by Lites et al. 1989, illustrated in Fig. 4) is adopted. For the reason stated in Paper I, the total optical depth scale τ is transformed to $\log_{10}\tau_0$ according to equations (26, 27) in Paper I.

First, the magnetic field vector is set to be $\boldsymbol{H}(1500\,\mathrm{G}, 60°, 30°)$ throughout all the depths, the resulting Zeeman splitting is 32.80 mÅ while the Doppler width ranges from 26.49 mÅ (at $\log_{10}\tau_0 = 3.427$) to 60.12 mÅ (at the surface) according to the model atmosphere. It is easily understood that no line splitting occurs in the emergent Stokes I profile as shown in Fig. 5 (a) (the dashed curve), where the curve computed in the null magnetic field case (the solid line) is also plotted for comparison. The effect of the field on the Stokes I profile shows up in the line broadening due to the line absorption enhancement from ±60 mÅ to about ±170 mÅ and the reduction in the interval (–60 mÅ, 60 mÅ). This says that the magnetic field not only increases the opacity at some wavelengths, but also decreases it at some other wavelengths. Stokes Q, U, V profiles (dash-dotted curves) in Fig. 5 (b)–(d) again show their normal shapes.

Again, we plot the CF_I and $\mathrm{CF}_{R;I}$ curves of sample wavelengths obtained in the null magnetic field case in Fig. 6 for an easy evaluation of the influence of magnetic field by comparison.

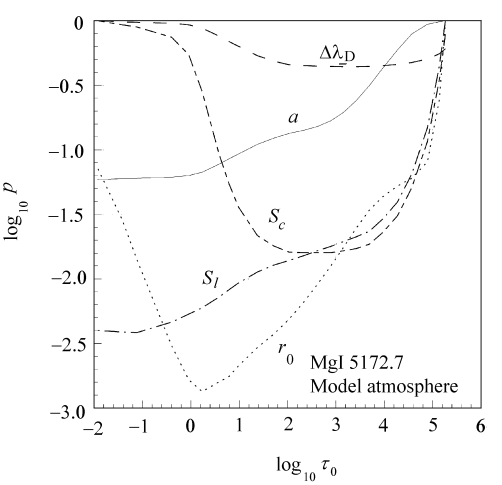

Fig. 4 The MgI 5172.7 model atmosphere of sunspot umbra. The curves represent distribution of logarithms of $p = a/a_{\max}$ (solid line), $\Delta\lambda_D/\Delta\lambda_{D;\max}$ (dashed line), $r_0/r_{0;\max}$ (dotted line), $S_l/S_{l;\max}$ (dash-dotted line), and $S_c/S_{c;\max}$ (long-short line) respectively.

Now let us watch what happens to the formation region when the magnetic field is inserted into the model atmosphere. First, we still care about whether it influences the formation region of the line core. One can see from Fig. 7 (a) that the formation regions of wavelengths within the line core of $|\Delta\lambda| \leq 30$ mÅ are the same, though stretched a little downward. Thus the line formation core still stands. Its formation regions range from $\log_{10}\tau_0 = -1.413$ to 1.717. The variation of the formation regions becomes more and more marked from $|\Delta\lambda| = 40$ mÅ

to 60 mÅ where the formation region broadening shows up most clearly in both the CF_I and $\mathrm{CF}_{R;I}$ curves, e.g., the dotted line ($\Delta\lambda = 60\,\mathrm{m\AA}$). Beyond 120 mÅ (say, 200 mÅ, the thick solid line), the non-magnetic field behaviour is seen once again in both CFs.

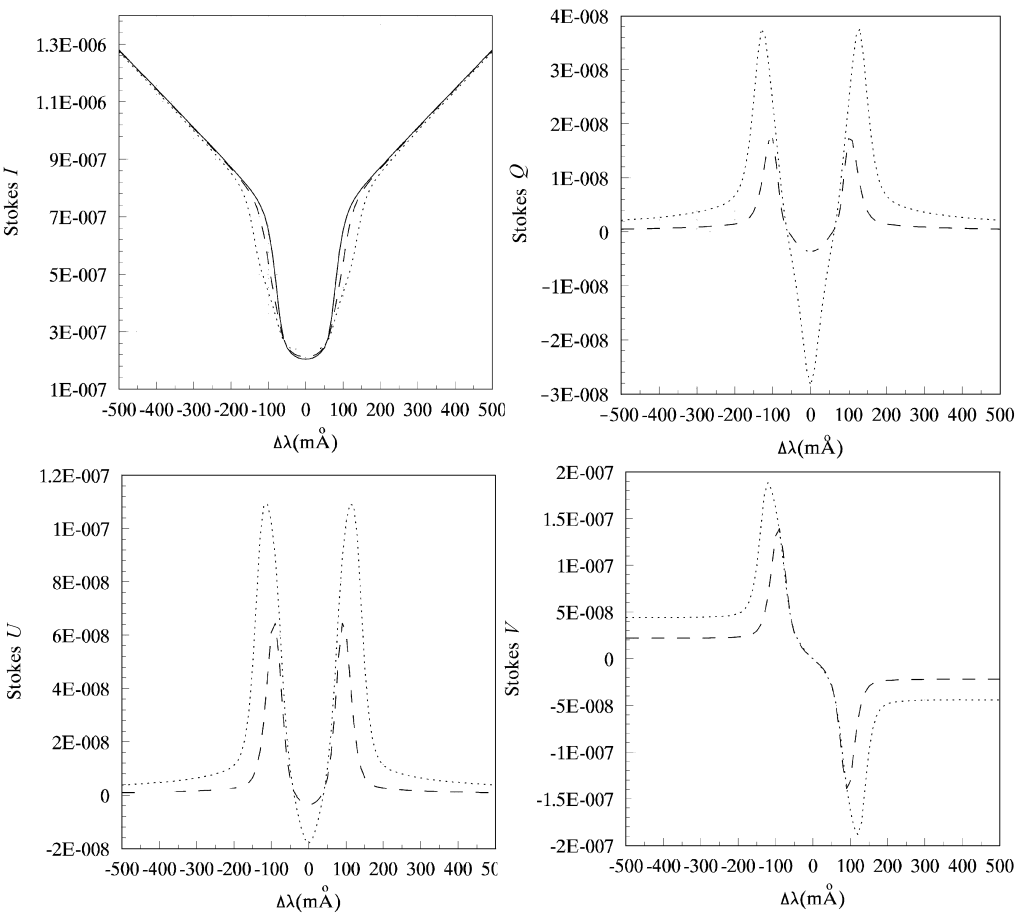

Fig. 5 The Mg I 5172.7 synthetic Stokes I, Q, U, V profiles emerging from the model atmosphere specified in Fig. 4 with null magnetic field (solid line), a weak field $\boldsymbol{H} = (1500\,\mathrm{G}, 60^\circ, 30^\circ)$ (dash-dotted line), and a strong field $\boldsymbol{H} = (3000\,\mathrm{G}, 60^\circ, 30^\circ)$ (dotted line). All the intensities are in units of $\mathrm{erg\,s^{-1}\,cm^{-2}\,sr^{-1}\ Hz^{-1}}$. Note that the specific intensity is increased in the line core when the magnetic field is present. In the strong field case, the line is partially split (dotted line) in the line core. Stokes Q, U, V profiles show their normal shapes and one can see their sensitivity to the magnetic field strength when the magnetic field strength is above a certain level.

Turn our attention now to the formation issue of the polarization states of the escape photons. By comparing to the simple 11-layer model, the depth distribution of the escape line photons with given definite polarization state becomes more complicated. For example,

the formation regions of different bands become separate, i.e., they are wavelength dependent. However, one can find that at each wavelength, Stokes Q, U, V form in the same region as does Stokes I.

Generally, the formation regions of the peaks or valleys of Stokes Q, U, V profiles (π and σ components) in the line wings (± 100 mÅ for Q, ± 90 mÅ for U, V in this case) are assumed to represent their formation region. Let us watch whether it possesses a special feature that enables such a selection to be made for this line. From both CF_Q and $\mathrm{CF}_{R;Q}$, the Stokes Q peak ($\Delta\lambda = 100$ mÅ) forms in the vast region from the middle layer of the chromosphere down to the middle layer of the photosphere, rather than only in the chromosphere. The same is the case for Stokes U and V. Therefore, the formation regions of those special wavelengths contain a wide range but not all the layers where both the line absorption and magnetic field are present. This may be the only feature they show.

The designed magnetic field above is not so strong that no line splitting occurs. When the magnetic field strength gets to 3000 G while the field angles keep unchanged, the Stokes I profile shows a doublet in the line core (see the dotted curve in Fig. 5(a)), with the valleys locating at ± 30 mÅ. Fig. 8 depicts the $\mathrm{CF}_{I,Q,U,V}$ curves of sample wavelengths, while the curves of CF_R are not plotted because their behaviour is similar, as is seen in Fig. 7. The most evident variation in Fig. 8 compared to Fig. 7 occurs in CF_I. The formation region of the line center of Stokes I (from $\log_{10}\tau_0 = -1.413$ to 3.162) is broadened more than those of $\Delta\lambda = \pm 20, 30$ mÅ (from $\log_{10}\tau_0 = -1.413$ to 2.617 and from -1.413 to 1.717 respectively). This means that within the line core there are no one set of wavelengths whose width is comparable to the depth-average of Doppler width forming in the same depth range, or the line formation core disappears. The formation regions of other wavelengths such as $\Delta\lambda = 110, 120$ mÅ (dash-dotted and long-short lines) are shifted to deeper layers. The same situation exists in the formation regions of the polarization profiles. For example, the Stokes Q of line center forms in the depth interval $(-1.116, 3.162)$ and the formation region of $\Delta\lambda = \pm 10$ mÅ is $(-1.116, 2.893)$, that of ± 20 mÅ is located in $(-1.116, 2.617)$, and ± 30 mÅ, in $(-1.116, 1.717)$ (cf Fig. 8(b)). On the other hand, the feature that keeps unchanged is that the Stokes Q, U and V form in the same region at the same wavelength (cf Fig. 8 (b)–(d)), and the region agrees with that of Stokes I, though their peaks are not always located at the same depth. For the peaks or valleys of Stokes Q, U, V

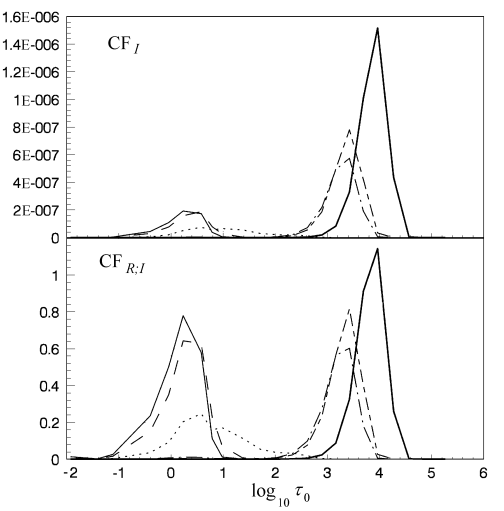

Fig. 6 The sample CF_I and $\mathrm{CF}_{R;I}$ curves in the null magnetic field case. The unit of CF is erg s^{-1} cm^{-2} sr^{-1} Hz^{-1} while $\mathrm{CF}_{R;I}$ is dimensionless. The types of curves correspond to CF_I and $\mathrm{CF}_{R;I}$ at wavelength displacements from line center respectively: 0 mÅ (thin solid line); 30 mÅ (dashed line); 60 mÅ (dotted line); 90 mÅ (dash-dotted line); 100 mÅ (long-short line); and 200 mÅ (thick solid line) respectively.

in the line wings (± 130 mÅ, ± 110 mÅ, ± 120 mÅ, respectively), their formation regions spread over the intervals $(2.617, 4.890)$, $(1.717, 4.571)$, $(2.032, 4.890)$, respectively. In this case, they do not show the feature that they cover the widest depth range.

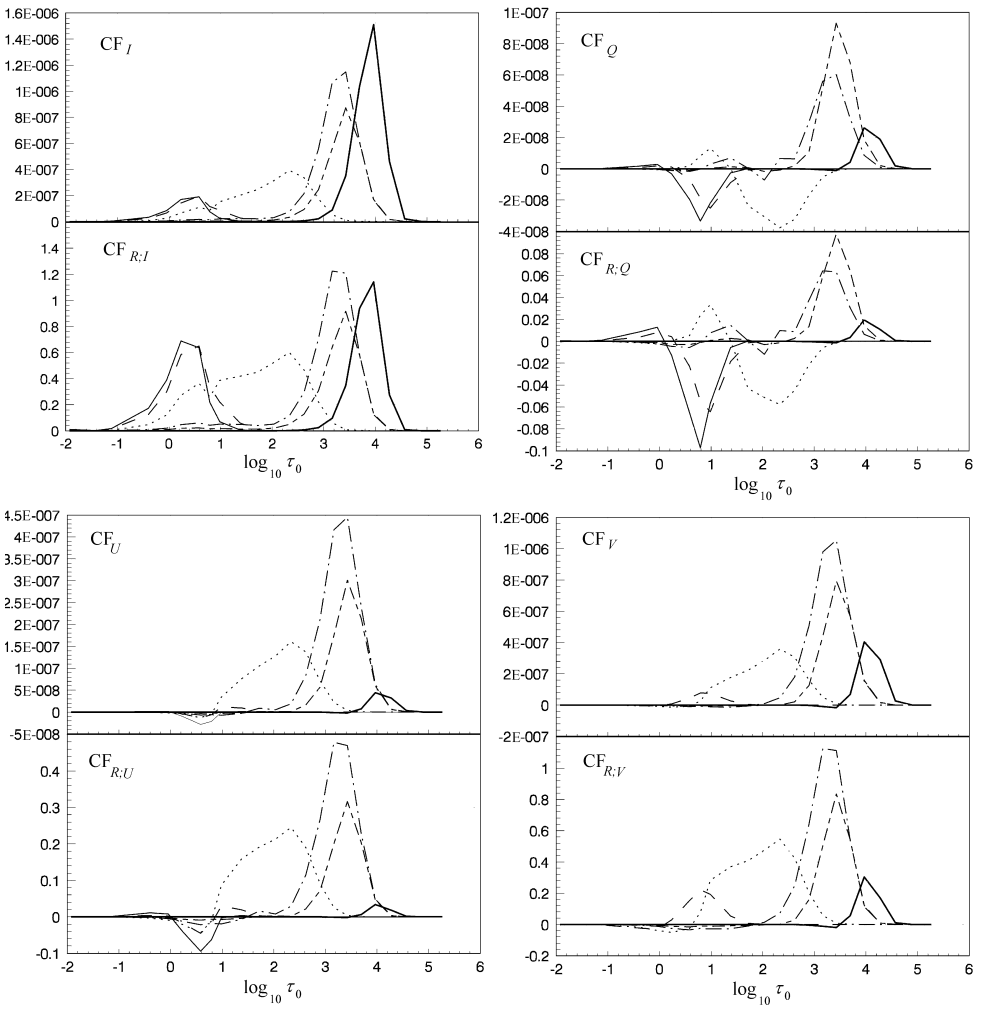

Fig. 7 The wavelength-dependence of the sample Mg I 5172.7 Stokes CF and CF$_R$ curves in a solar model umbral atmosphere with a weak field $\boldsymbol{H} = (1500\,\mathrm{G}, 60^\circ, 30^\circ)$. The unit of CF is erg cm^{-2} s^{-1} sr^{-1} Hz^{-1}, while CF$_{R;I}$ and τ_0 are dimensionless. The types of curves corresponding to CF$_{I,Q,U,V}$ and CF$_{R;I,Q,U,V}$ at wavelength displacements from line center respectively are the same in Fig. 6. Note that the formation regions of Stokes Q, U, V are now wavelength-dependent. However, they cover the same region at each wavelength within the line band, as those of Stokes I.

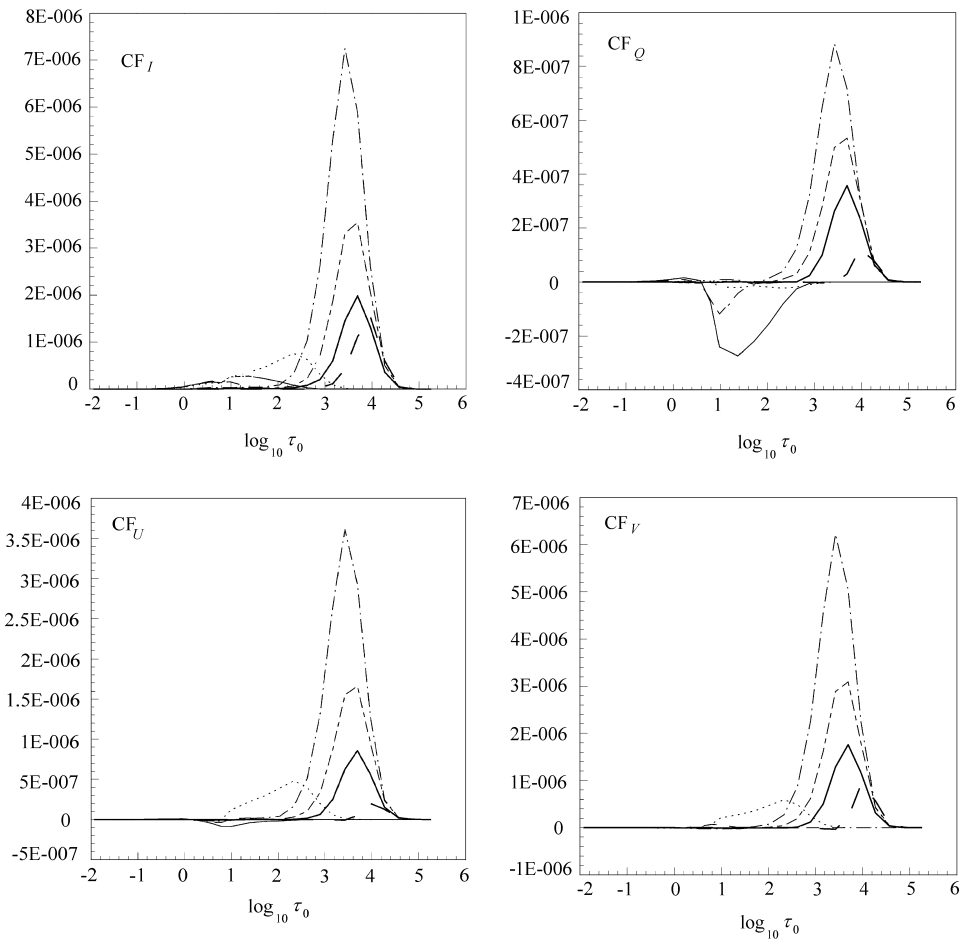

Fig. 8 The wavelength-dependence of the sample Mg I 5172.7 Stokes $\mathrm{CF}_{I,Q,U,V}$ curves in a solar model umbral atmosphere with a strong field $\boldsymbol{H} = (3000\,\mathrm{G}, 60^\circ, 30^\circ)$. The unit of CF is the same as in Fig. 7. The types of curves corresponding to $\mathrm{CF}_{I,Q,U,V}$ at wavelength displacements from line center respectively are: 0 mÅ (thin solid line); 30 mÅ (dashed line); 60 mÅ (dotted line); 110 mÅ (dash-dotted line); 120 mÅ (long-short line); 130 mÅ (thick solid line); and 200 mÅ (thick dashed line). Note that Stokes I formation regions of line center is wider than that of $\Delta\lambda = 20$, 30 mÅ. This signifies the line formation core disappears.

Finally we change only the magnetic field angle parameters while the strength is kept at $H = 3000\,\mathrm{G}$ in the same model atmosphere. For example, let

$$\gamma = (24.0 - n) \times 2^\circ, \;\; \chi = n \times 3^\circ. \tag{18}$$

Where n signifies the grid ($n = 1$ for surface and $n = 24$ for the bottom of the photosphere). In this situation the line splitting disappears because of the decrease in the field inclination

and hence in the σ component. The line formation core re-appears and its wavelength width becomes 40 mÅ (not plotted). Its formation region ranges from $\log_{10}\tau_0 = -1.413$ to 2.331, wider than that in the no or weak magnetic field cases, but narrower than the line center formation domain in the previous case. It is found again that though the field angles are depth dependent, all the Stokes parameters still form in the same region at the same wavelength.

4 APPLICATION TO THE SOLAR UNPOLARIZED AND POLARIZED FILTERGRAMS

The main purpose of the paper is to better understand the line formation process in stellar magnetized atmosphere. In fact, the above observation is instructive to the solar unpolarized and polarized filtergrams obtained by the filter-type magnetographs which measure the accumulation of the received line photons and their polarization states of wavelengths within the bandpass used. The CF for this situation can be suitably expressed by

$$\mathrm{CF}' = \frac{\int_{\lambda_{0,\mathrm{bp}}-\Delta\lambda_{\mathrm{bp}}/2}^{\lambda_{0,\mathrm{bp}}-\Delta\lambda_{\mathrm{bp}}/2} \mathrm{CF}(\lambda)\mathrm{d}\lambda}{\Delta\lambda_{\mathrm{bp}}}. \tag{19}$$

Where $\Delta\lambda_{\mathrm{bp}}$ is the bandpass used and $\lambda_{0,\mathrm{bp}}$ its wavelength center.

For $\mathrm{CF}_I^{'}$, as pointed out, it informs us where the escape or received line photons come from, so one obtains the depth redistribution of these photons. This provides a possibility of reconstructing the three-dimensional images of the observing area from serial and unblended bandpass observations from the line center to the far wings. We have carried out such a procedure in another paper in the unpolarized case.

For the Stokes polarized filtergrames, we need both $\mathrm{CF}_{R;Q,U,V}^{'}$ and $\mathrm{CF}_{Q,U,V}^{'}$ curves. The former announce us where the corresponding polarization states form, especially for the magnetic canopy-like structure case, and the latter tells us equivalently how many received line photons own the corresponding polarization states. Following the procedure just outlined, one may get the Stokes polarization image of each relevant layer. However, this task is more difficult than the reconstruction of the three-dimensional image of received line photons from $\mathrm{CF}_I^{'}$, because the stratification of the magnetic field is very difficult to determine exactly. Up to date there is no mature model polarized atmosphere in the literature. On the other hand, it is worth noting that from these layer images one cannot exactly derive the information about the physical conditions in the layer, as pointed out above. Though what one obtains is only quantified morphology, it nevertheless gives us some information needed in further studies.

5 DISCUSSION AND CONCLUSIONS

The clue of the line formation region variation due to the presence of magnetic field can be directly found by comparing the non-magnetic and magnetic Stokes I profiles. Such variation generally occurs in those influenced wavelengths in the manner that the stronger the field strength is, the wider wavelength range is involved. The line formation core, introduced in Paper I, disappears only when the magneto-induced line splitting occurs in the line core, otherwise it keeps its virtue that its formation region can be used to define the line formation region.

We have seen that in the tenuous atmosphere with restricted distribution of line absorption and constant vector magnetic field, all the wavelengths of Stokes polarization profiles form in

the same regions where both the line absorption and magnetic field are present. On the other hand, the formation region of the Stokes I spectrum does not have this property. In the opaque atmosphere with ubiquitous line absorption and magnetic field, as in the model atmosphere and field stratification accepted in this paper, the formation regions move to deeper layers as the wavelengths go towards the line wings, compared with the field-free case. However, the feature remains that all the Stokes parameters of the same wavelength form in the same region in the real magnetized atmosphere for Mg I 5172.7, even when the field angles vary with depth. The formation regions of the peaks or valleys in the line wings of the Stokes polarization profiles (σ and π components) generally show the feature that they cover the vastest region where both the line absorption and magnetic field are present. If they are assigned to the formation regions of the corresponding Stokes polarization profiles, this is the meaning they have.

In Paper I and this paper, we only consider one real line, i.e., Mg I 5172.7 which was formed in the solar umbral model atmosphere approximating reality. This line may be the representative of one kind of lines formed in the solar umbral chromosphere in the sense that their formation regions are represented by the formation regions of their line formation cores. Some of the above conclusions may not hold for lines formed in the photosphere.

One significant aspect of this work lies in the explanation of the solar unpolarized and polarized filtergrams.

Acknowledgement This series of papers is sponsored by the Project 19976301 and Major Project 19791090 of the National Natural Science Foundation of China.

References

Landi Degl'Innocenti E., 1976, A&AS, 25, 379
Larsson B., Solanki S. K., Grossman-Doerth U., 1990, In: L. November, ed., Proc. 11th NSO Sacramento Peak Summer Workshop, Solar Polarimetry, p.479
Lites B. W. et al., 1988, ApJ, 330, 493
Qu Z. Q., 1997, PhD thesis, Yunnan Astronomical Observatory, Chinese Academy of Sciences
Qu Z. Q., Zhang X. Y., Gu X. M., , 1999, MNRAS, 305, 737 (Paper I)
Rees D. E., Murphy G. A., Durrant C. J., 1989, ApJ, 339, 1093 (RMD)
Ruiz Cobo B., del Toro Iniesta J. C., 1994, A&A, 283, 129
Sánchez Almeida J. et al., 1996, A&A, 314, 295